

GLANCING INCIDENCE OPTICS FOR X-RAY AND ULTRAVIOLET ASTRONOMY

J. H. UNDERWOOD and W. M. NEUPERT

Solar Plasmas Branch, NASA-Goddard Space Flight Center, Greenbelt, Md., U.S.A.

and

R. B. HOOVER

Astronomics Laboratory, NASA-Marshall Space Flight Center, Huntsville, Ala., U.S.A.

Abstract. Glancing incidence telescopes of the kind first described by Wolter have now been physically realized, so that it is now possible to obtain high resolution images of celestial objects at all wavelengths greater than about 3 Å. In this paper we shall describe two such instruments: the GSFC-MSFC X-ray telescope for the Apollo telescope mount uses Wolter type 1 optics and is capable of forming images of the sun in the 8–70 Å region with spatial resolution of the order of one arc second. The GSFC extreme ultraviolet spectroheliometer for OSO H uses type 2 optics and can obtain images of the Sun in spectral lines in the 170–400 Å region with a spatial resolution of about ten arc seconds. Theoretical (ray trace) and laboratory data on these systems will be presented.

In this paper we shall describe two instruments which have been built to observe the Sun with high spatial resolution, the first in the soft X-ray region (8–70 Å) and the second in the extreme ultraviolet region (170–400 Å). Both of these instruments employ glancing incidence optics of the type proposed by H. Wolter in 1952, and which use two conic sections of revolution to satisfy the Abbé sine condition approximately. Figure 1 shows schematically the two types of telescope. The first is the well known type 1 or inside-inside system which has, as Dr Giacconi described, been successfully used by both AS and E and ourselves to photograph the Sun in the X-ray region. The second is the type 2 or stretched-out Cassegrain system which we are using in our EUV spectroheliometer on OSO H.

The first instrument we shall describe is the S056 X-ray telescope which is being built to fly in the ATM section of NASA's Skylab. This is a joint GSFC-MSFC experiment, with Mr J. E. Milligan the principal investigator, and the hardware is being built and tested at MSFC. Figure 2 is a schematic diagram of the optical layout of the S056 instrument. The angle of glancing incidence is 54 arc min on both reflecting surfaces, and the diameter of the conic sections at the plane of intersection is 22.5 cm. Once these parameters have been determined for a particular telescope, the instrument almost designs itself: there is very little freedom left to adjust the other parameters to improve the imaging, although the length of the elements may be changed to alter the collecting area. The focal length of this instrument is 190 cm and the collecting area 14.8 cm², giving an *f*/44 system (neglecting reflection efficiency). This is adequate for the type of work we intend to do on the ATM: the study of the morphology of the solar corona, active regions and X-ray flares with high spatial and time resolution. The solar images will be recorded on film, and coarse spectral resolution will be provided by filters of thin plastic and metal. Figure 3 shows the instrument mounted in the ATM rack.

In Figure 4 we see two different mechanical designs for the X-rays optics. In the first design the reflecting surfaces are of bare polished fused silica, in the second they are of 'Kanigen' coated beryllium. We had both of these designs made by the Perkin-Elmer Corporation in order to find the best method of construction and to evaluate

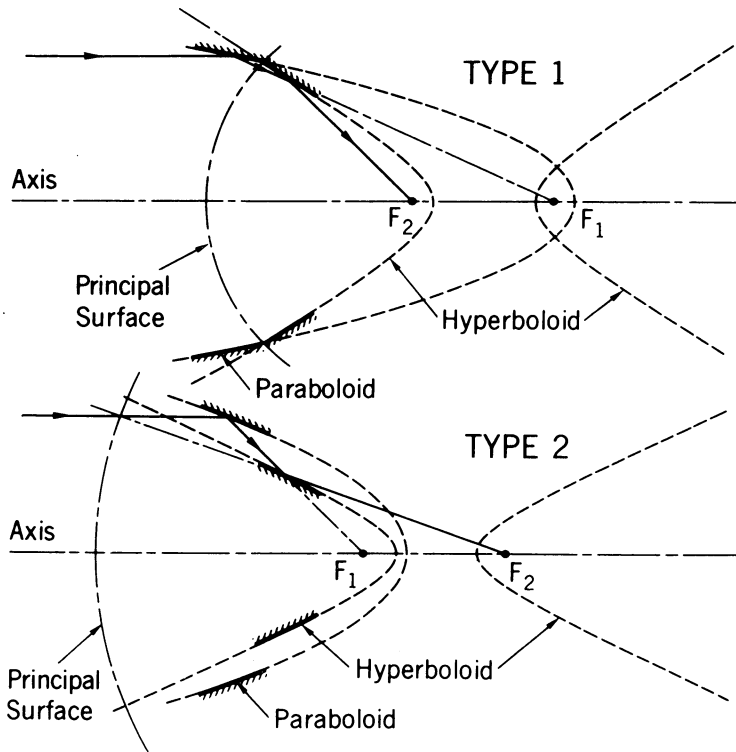


Fig. 1. Two types of X-ray telescope suggested by Wolter. Type 1 is used in the S056 X-ray telescope and type 2 in the OSO-H EUV spectroheliometer.

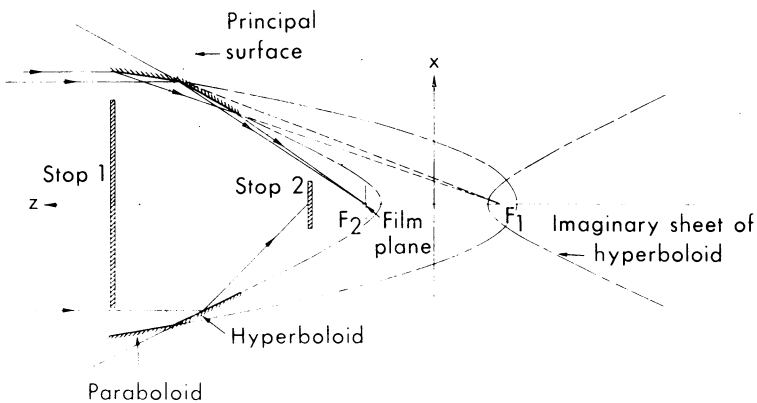


Fig. 2. Schematic diagram of optical system of S056 X-ray telescope.

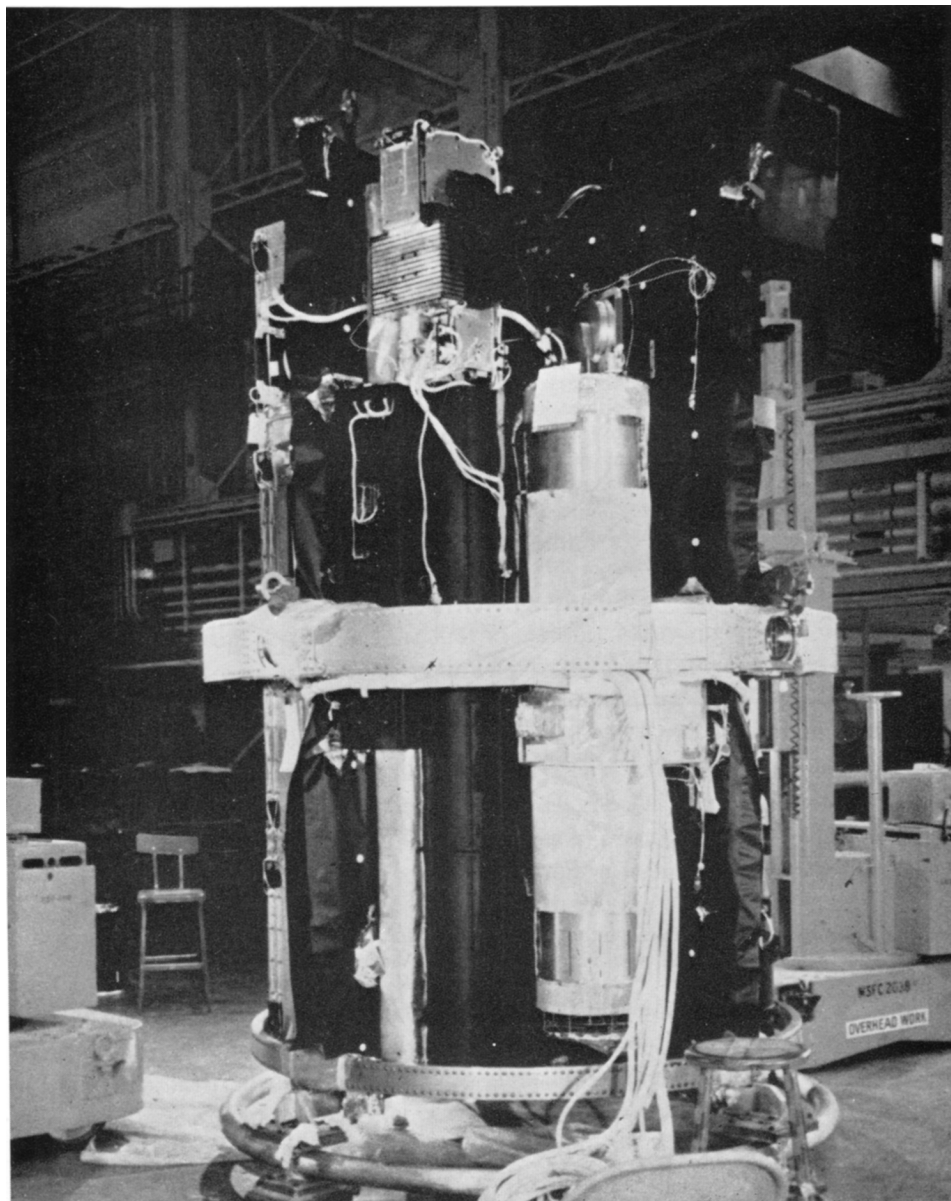


Fig. 3. S056 telescope mounted in ATM 'rack'. (White instrument near cables.)

the performance of the two different reflecting surfaces in the X-ray region. A fused silica telescope was also made in the optics shop at MSFC. The fused silica optics proved to be far superior, as the surfaces could be polished much smoother (on a microscopic scale) than could the 'Kanigen' coated surfaces. The test results we shall present were obtained with the fused silica optics. Figure 5 is a photograph of a fused

silica telescope, showing the optical elements mounted in their beryllium cell. In Figure 6 appear some spot diagrams, computed by ray tracing assuming perfect optical surfaces, i.e., no errors of figure or roughness. These spot diagrams show that we can expect good resolution over a field of view as large as, or slightly larger than, the solar disc. In practice the resolution attainable by the telescope is limited not by

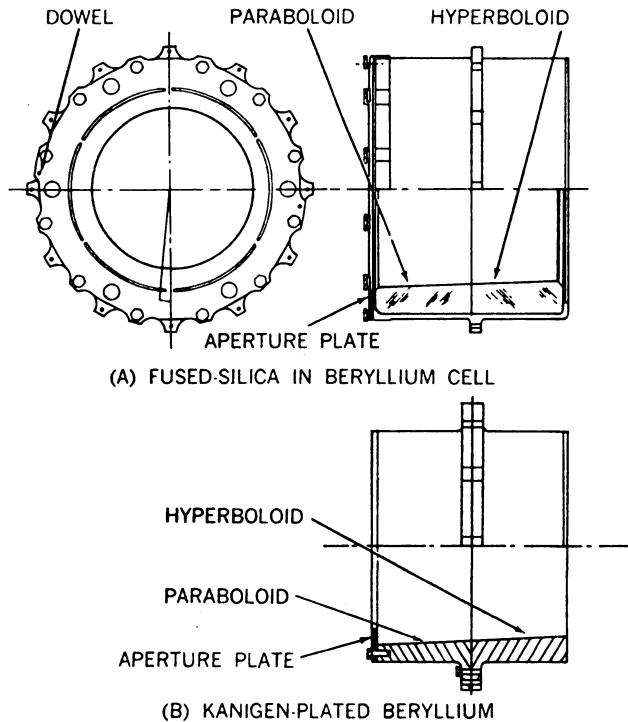


Fig. 4. Two methods of construction of S056 X-ray optics.

the optical imaging properties of the particular telescope design, but by errors introduced in the construction of the telescope, in particular, the microscopic roughness of the surface and the so-called 'regularity errors' or 'errors of figure' (Figure 7). In order to evaluate a particular telescope it is therefore necessary to test it in the laboratory with targets of known resolution and contrast. Testing in visible light is unsatisfactory as the surface errors (of both kinds) will obviously have a different effect at $\sim 5000 \text{ \AA}$ from the effect they have at $\sim 10 \text{ \AA}$. In addition, the diffraction from the annular aperture (which is 98% obscured in the case of our S056 telescope) makes visible light tests inadequate for evaluating telescope performance. We have therefore tested the telescopes in the X-ray region. One method we have used is to look at an X-ray source at the end of a long (61 m) vacuum tank. However, even at this distance the object is not sufficiently far away and so we have developed an alternative method (Figure 8), in which one telescope is used as a collimator for the X-rays. This test, as

an evaluation of surface quality, is a worst case as there are four reflections instead of two. All the tests we shall describe were made with this set-up.

Figure 9 shows photographs of a USAF target taken with visible light using two fused silica telescopes. These photographs, and the others which follow, are highly enlarged photomicrographs of the original test data. For 9(a) Kodak high resolution

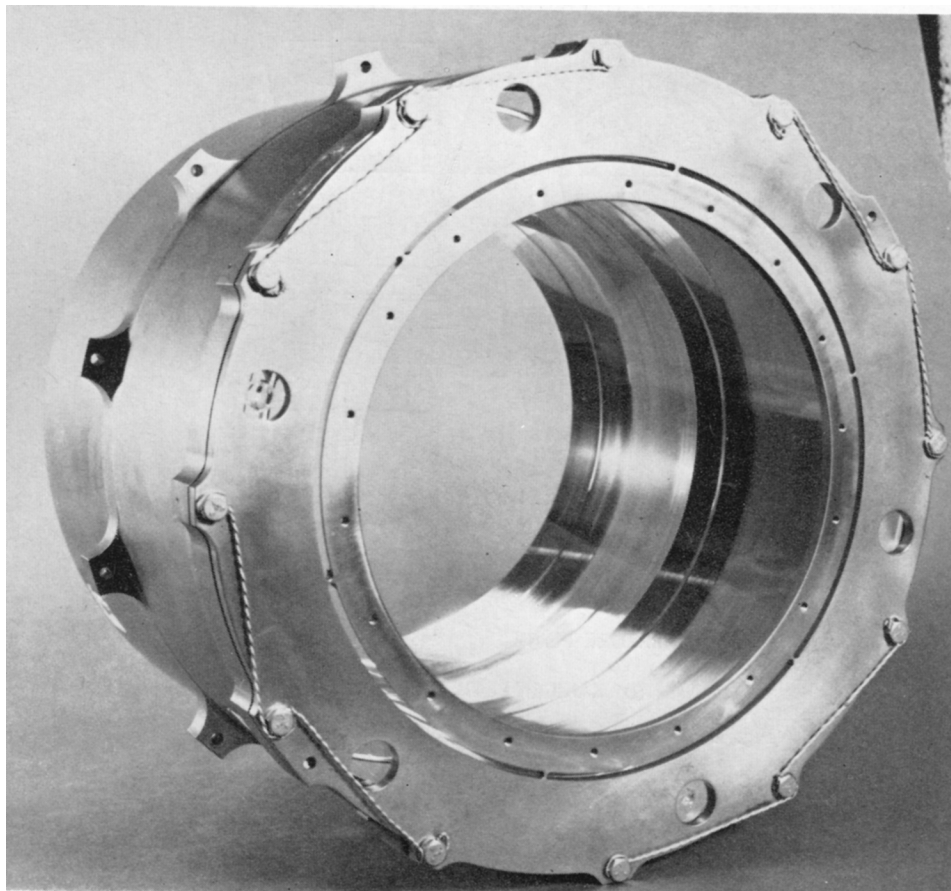


Fig. 5. X-ray mirror with reflecting elements of fused silica.

plate was used whereas for 9(b) the film was Kodak-114 (unsupercoated Panatomic-X). The latter is the film that will be used for the ATM mission. We see that in 9(a) the smallest resolvable bar targets (6.5) are separated by 1.0 s of arc, while in 9(b) only the 4.6 group can be seen, indicating a resolution of about 3.8 arc sec. (On the original negative the 5.3 group (2.7 s) may be seen.) The poorer resolution is evidently due to the increased graininess of the SO-114 film. Figure 10 shows the result of a test at 8 Å. SO 114 only was used during the X-ray tests as the high resolution plate has very low

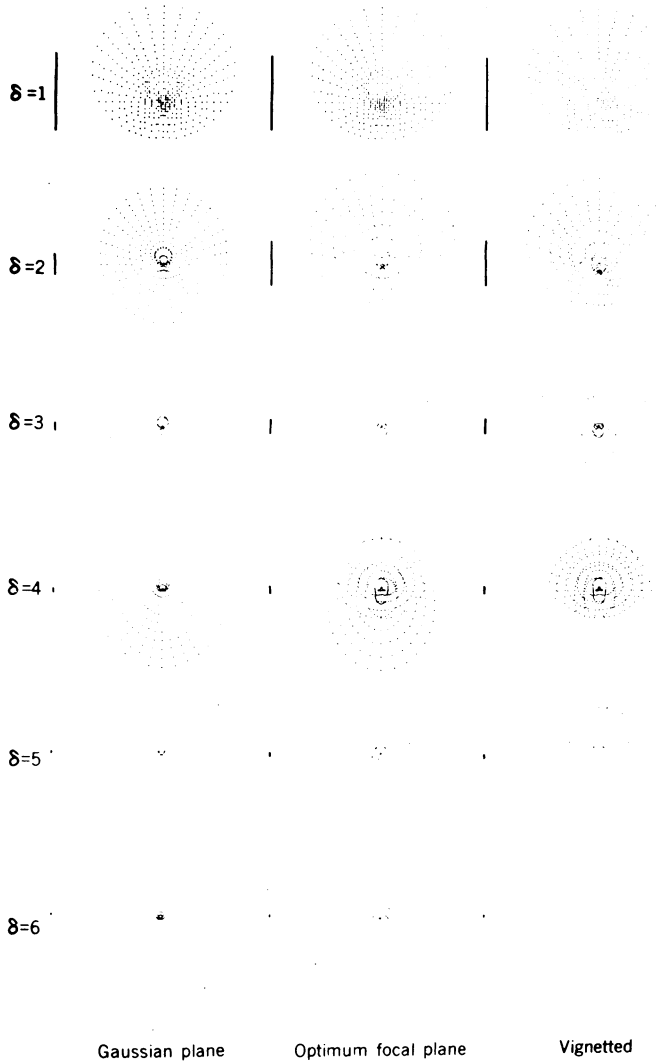


Fig. 6. Spot diagrams computed for the X-ray telescope. The β values represent milliradians off axis. The bars to the left of each spot diagram represent 1 arc sec.

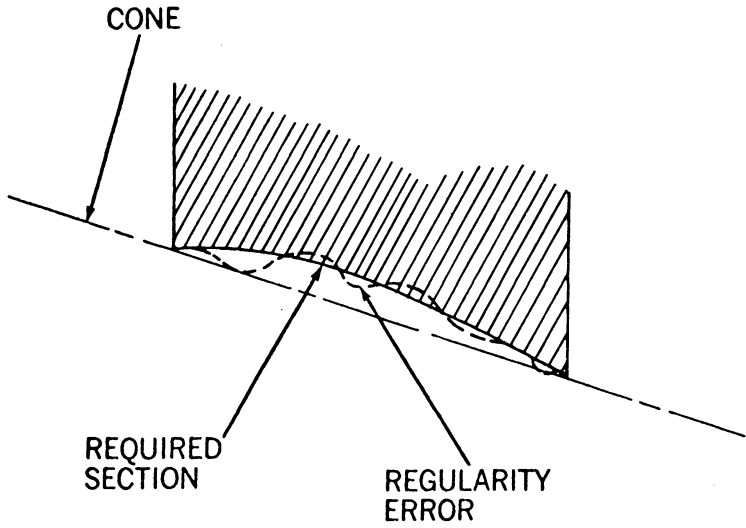


Fig. 7. The meaning of 'regularity error'.

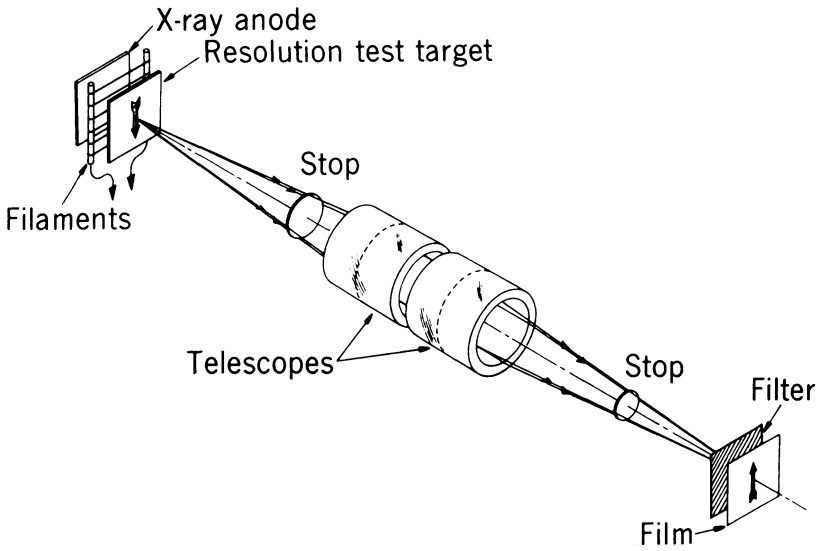


Fig. 8. Set-up for resolution testing in the X-ray region.

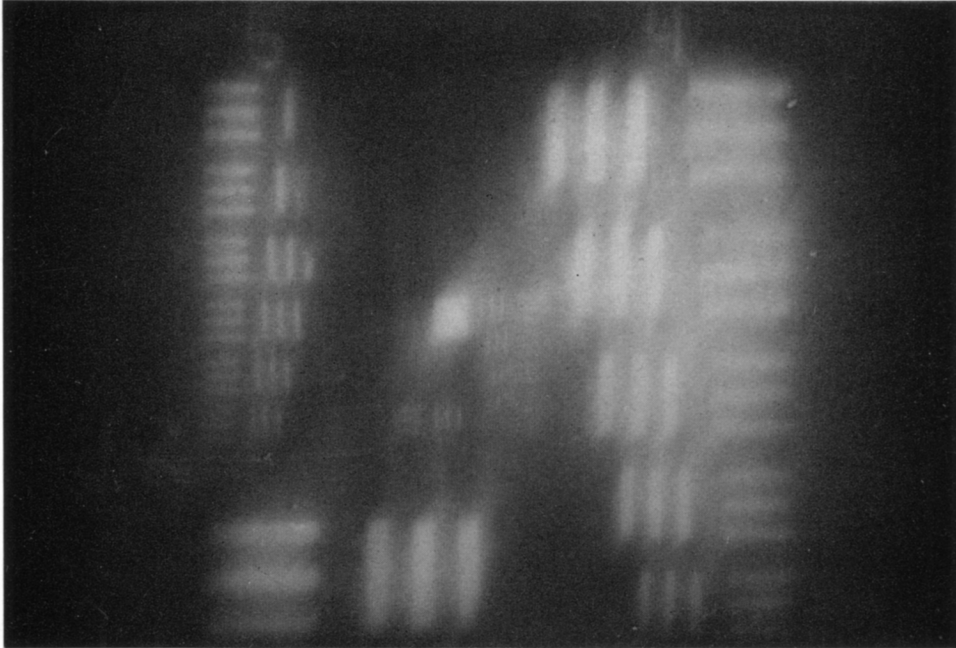


Fig. 9a.

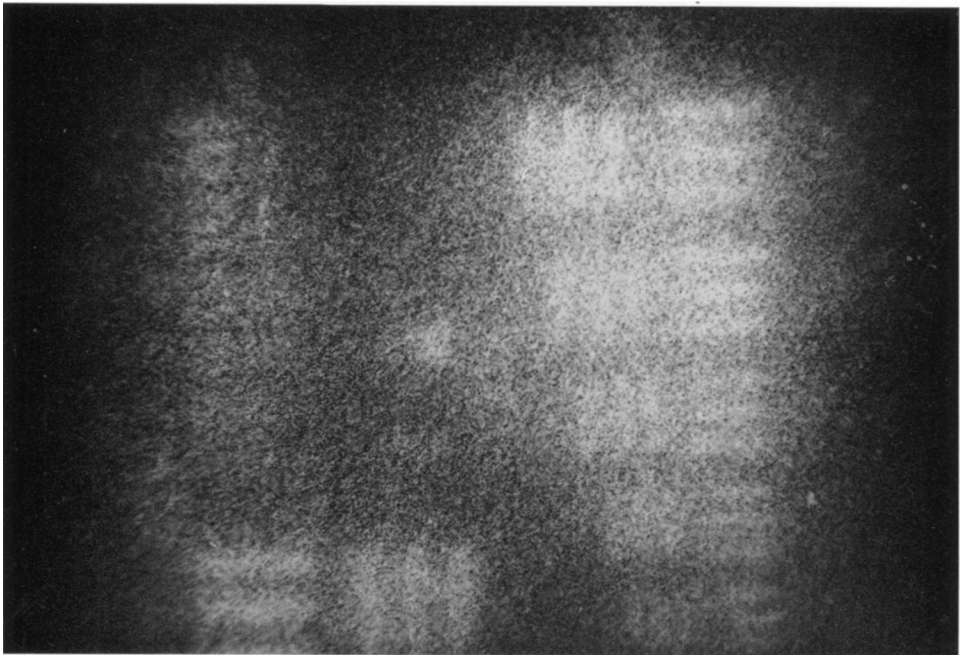


Fig. 9. a-b. USAF target photographed in visible light with two X-ray telescopes arranged as in Figure 8. (a) was taken using Kodak high resolution plate, (b) with SO-114 film.

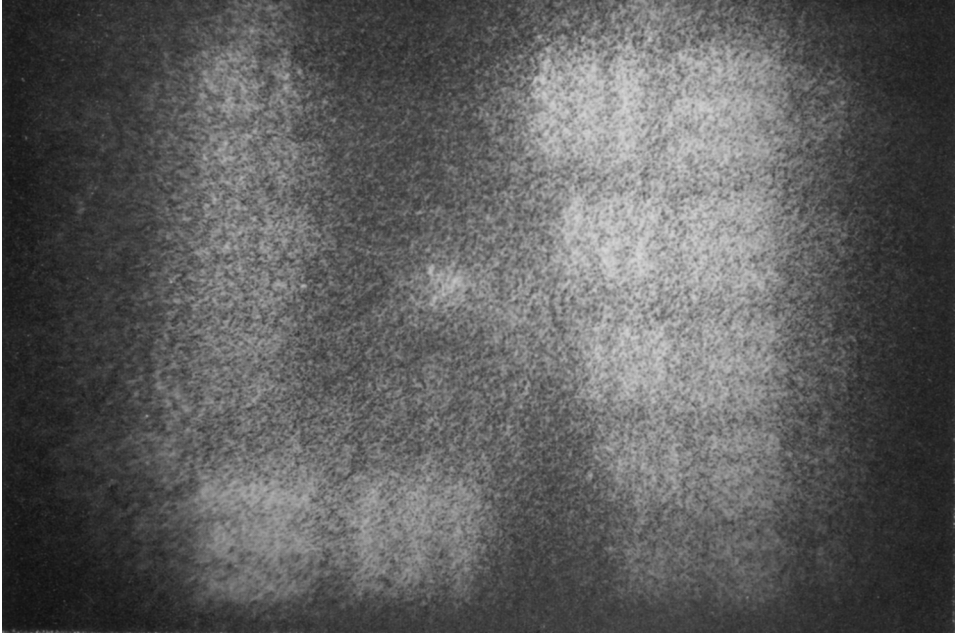


Fig. 10. 8 Å X-ray exposure on SO-114 film.

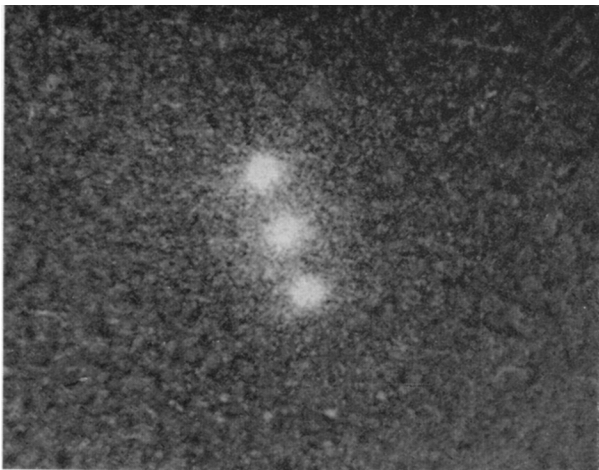


Fig. 11a.

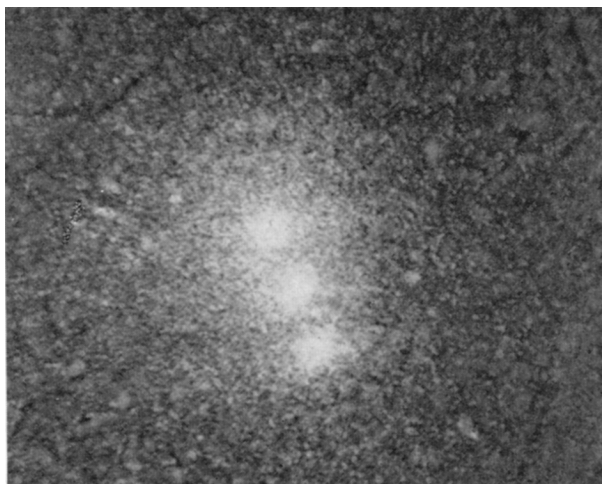


Fig. 11b.

Fig. 11a-b. 3-spot target photographed on SO-114 film (a) in visible light (b) in 8 Å X-rays.

sensitivity to X-rays. In 10 the same group (4.6) can still be seen indicating an X-ray resolution similar to that seen in visible light. We conclude from these tests that the ATM S056 X-ray telescope will be resolution limited at around 2–3 arc sec by the film used.

Figure 11 shows results with a different kind of test target, 3 dots with a separation center-to-center of 11 arc sec and a diameter of 5 arc sec. 11(a) was taken in visible light and 11(b) in 8 Å X-rays. Some scattering may be seen around the X-ray images but it is small and, taking into account the fact that these photographs were taken using *four* surfaces, the results seem to augur well for the future of this type of X-ray telescope.

We shall now describe briefly the EUV spectroheliometer we shall be flying on OSO H. This instrument operates in the range 170–400 Å and employs Wolter type 2 optics in the configuration shown in Figure 12. An image of the Sun in all wavelengths above 170 Å is formed in the focal plane of the telescope which has 85 cm focal length and 11 cm² collecting area. The telescope, which has bare fused silica reflecting surfaces, has a reflectivity of about 40% at 304 Å. A slit in the focal plane serves to define the region of interest on the Sun's disk and also to act as the entrance slit of the glancing incidence spectrometer of conventional type. Figure 13 shows the actual layout of the instrument. (Note that the physical layout is slightly different, and that a small Ebert-Fastie spectrometer has been substituted for the H α interference filter.) Figure 14 shows some computed spot diagrams for the EUV telescope. Again, we see that the off-axis resolution, although poorer than the resolution on axis, is still acceptable over a field of view as large as the Sun. In fact we hope to obtain a spatial resolution of around 10 arc sec and a spectral resolution of 1 Å with this instrument. This will enable us to construct images of the Sun in selected lines in the EUV by scanning the

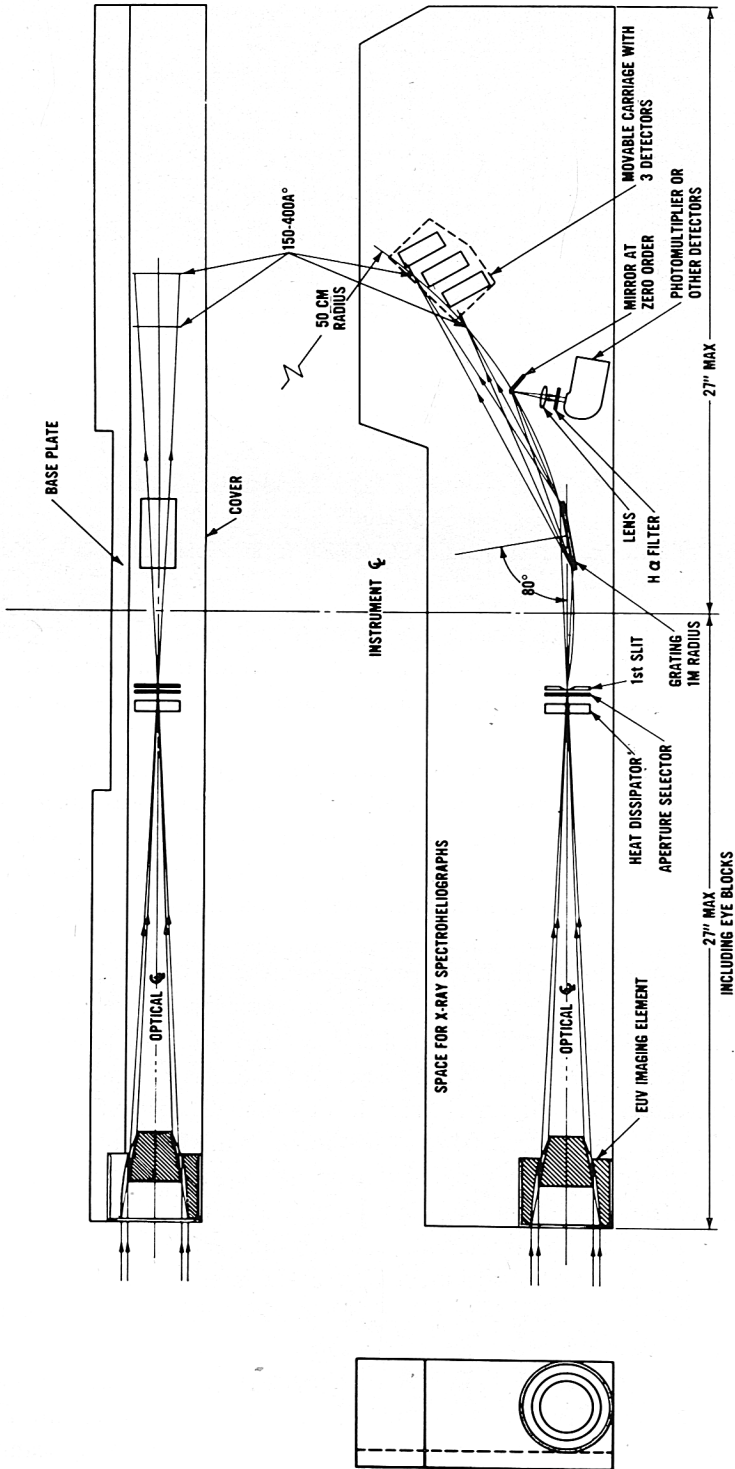


Fig. 12. Schematic diagram of OSO-H spectroheliometer.

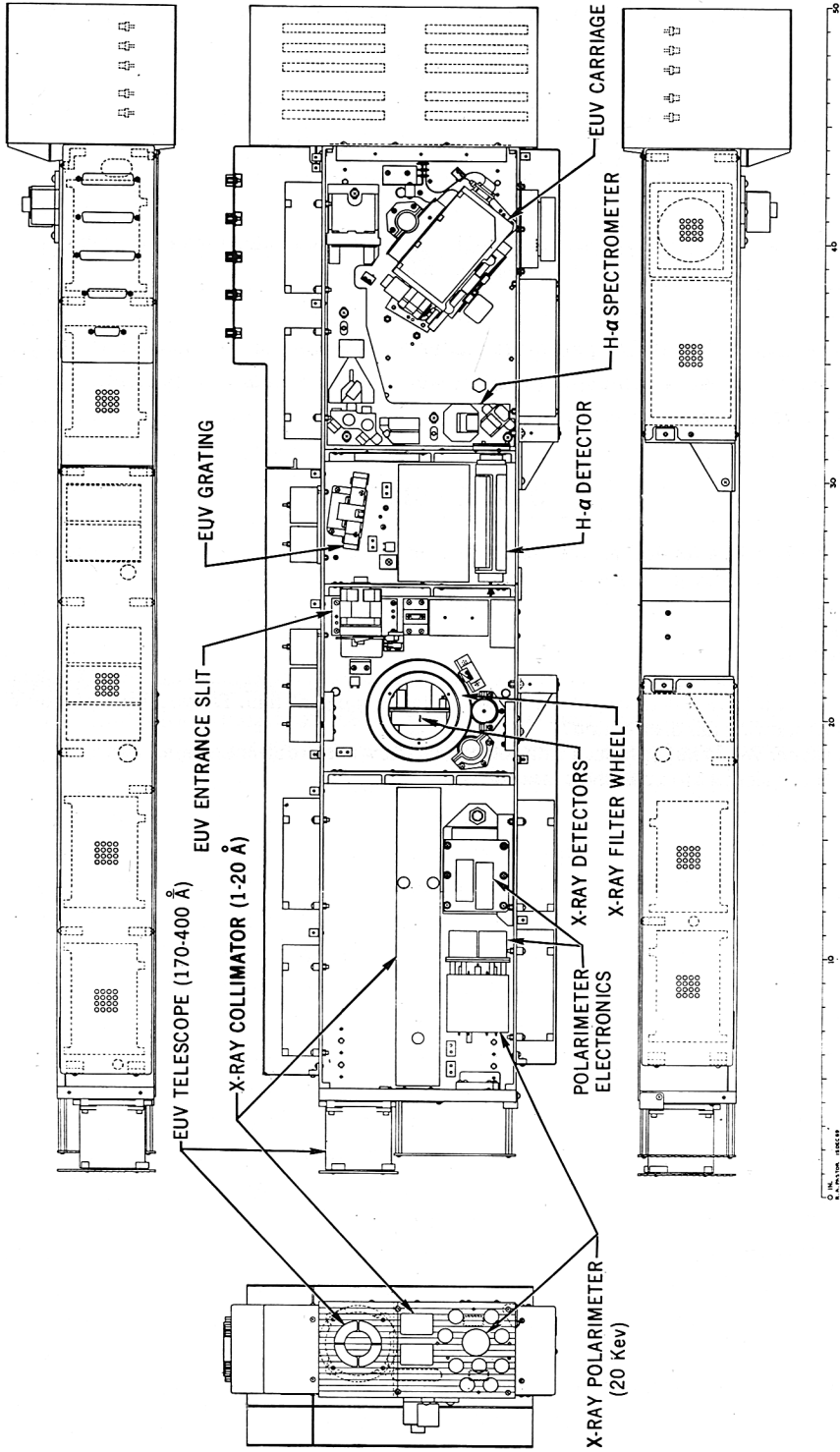


Fig. 13. OSO-H instrument housing component layout.

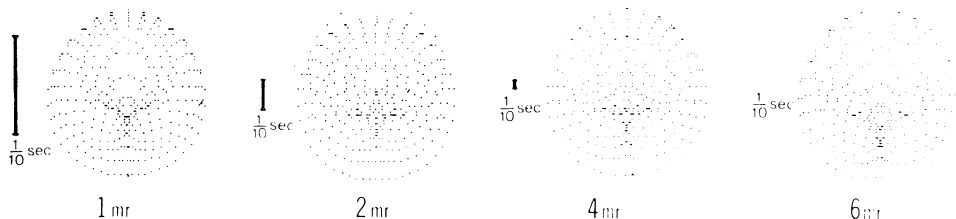


Figure 14. Spot diagrams for OSO-H EUV telescope plotted for various half field angles in milliradians.

instrument using the OSO spacecraft raster mode, and so to investigate physical processes in the solar chromosphere and lower corona, where the spectral lines in the 170–400 Å wavelength region are formed.

DISCUSSION

A. Hammerschlag: The residual aberrations in your telescopes do they come from errors in the individual mirrors or from errors in alignment between the two mirrors?

J. Underwood: Both. The surfaces must be accurately figured and accurately aligned. The alignment tolerances are in the micron range for relative translations of the elements and in the arc second range for their relative angular positioning.

R. Giacconi: The relative intensity distribution vs distance from center of image in focal plane as measured by film is very deceiving due to small dynamic range of film. Do you have proportional counter data showing this distribution?

J. Underwood: We do not have such data yet, but we know this problem exists, and we are at present setting up the equipment to make these measurements.